Front. Environ. Sci. Eng. 2022, 16(10): 127
https://doi.org/10.1007/s11783-022-1562-3

RESEARCH ARTICLE

Phylogenetic diversity of NO reductases, new tools for *nor* monitoring, and insights into N_2O production in natural and engineered environments

Sung-Geun Woo (✉)[1,2], Holly L. Sewell[1], Craig S. Criddle[1,2]

1 Department of Civil and Environmental Engineering, Stanford University, Stanford, CA 94305, USA
2 NSF Engineering Research Center, Re-Inventing the Nation's Urban Water Infrastructure (ReNUWIt), Stanford University, Stanford, CA 94305, USA

HIGHLIGHTS

- 548 representative *nor* genes were collected to create complete phylogenetic trees.
- The distribution of *nor* and *nod* genes were detected in 18 different phyla.
- The most conserved amino acids in NOR were located adjacent to the active site.
- *nor*-universal and Clade-specific primers were designed, suggested, and tested.

GRAPHIC ABSTRACT

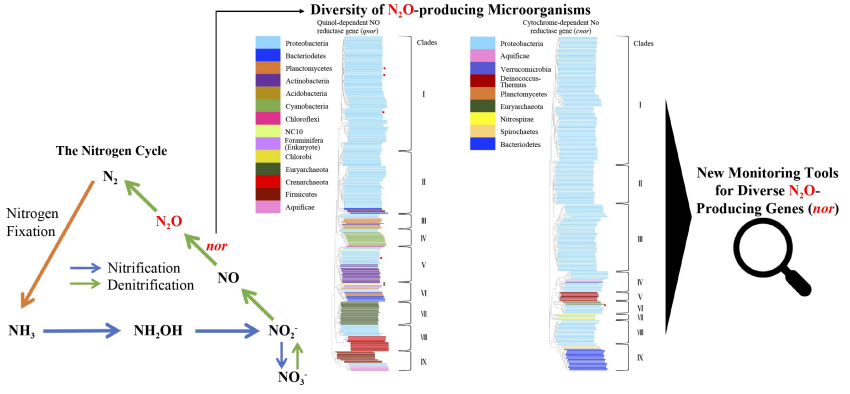

ARTICLE INFO

Article history:
Received 25 October 2021
Revised 28 January 2022
Accepted 31 January 2022
Available online 10 March 2022

Keywords:
N_2O
Greenhouse gas
NO reductase
NO dismutase
Primer
Crystal structure

ABSTRACT

Nitric oxide reductases (NORs) have a central role in denitrification, detoxification of nitric oxide (NO) in host-pathogen interactions, and NO-mediated cell-cell signaling. In this study, we focus on the phylogeny and detection of qNOR and cNOR genes because of their nucleotide sequence similarity and evolutionary relatedness to cytochrome oxidases, their key role in denitrification, and their abundance in natural, agricultural, and wastewater ecosystems. We also include nitric oxide dismutase (NOD) due to its similarity to qNOR. Using 548 *nor* sequences from publicly accessible databases and sequenced isolates from N_2O-producing bioreactors, we constructed phylogenetic trees for 289 *qnor*/*nod* genes and 259 *cnorB* genes. These trees contain evidence of horizontal gene transfer and gene duplication, with 13.4% of the sequenced strains containing two or more *nor* genes. By aligning amino acid sequences for *qnor* + *cnor*, *qnor*, and *cnor*, we identified four highly conserved regions for NOR and NOD, including two highly conserved histidine residues at the active site for qNOR and cNOR. Extending this approach, we identified conserved sequences for: 1) all *nor* (*nor*-universal); 2) all *qnor* (*qnor*-universal) and all *cnor* (*cnor*-universal); 3) *qnor* of *Comamonadaceae*; 4) Clade-specific sequences; and 5) *nod* of *Candidatus Methylomirabilis oxyfera*. Examples of primer performance were confirmed experimentally.

1 Introduction

One of the declared "Grand Challenges for Engineering in the 21st Century" is to manage the global nitrogen cycle (National Academy of Engineering, 2016). At present, N_2 fixation adds over 400 Tg of reactive nitrogen per year to terrestrial and marine ecosystems (Tian et al., 2020). About half this total is due to human activities, especially the energy-intensive Haber-Bosch process which, by itself, generates ~ 125 Tg of NH_3 per year (Fowler et al., 2013). Widespread NH_3 usage as fertilizer has led to increased nitrogen contamination of soils and groundwater, eutrophication of freshwater and estuarine ecosystems, and air pollution by NO_x, including nitrous oxide (N_2O) (Fowler et al., 2013). N_2O is a potent

✉ Corresponding author
E-mail: wsg135@stanford.edu

greenhouse gas and the most significant stratospheric ozone-depleting substance (Schreiber et al., 2012). It is largely produced by microbial reduction of nitric oxide (NO), a toxic free radical (Hu et al., 2019). Because its rate of production (~ 17 Tg N/year) exceeds its rate of removal (~ 13 Tg N/year), N_2O is accumulating in the atmosphere (~4 Tg N/year) (Tian et al., 2020).

Imbalances in atmospheric nitrogen are not limited to the Anthropocene and likely occurred in Earth's deep past. NO produced by volcanic lightning may have served as Earth's first deep electron acceptor (Navarro-González et al., 1998). In anaerobic ammonium oxidation (ANAMMOX) bacteria, NO reacts with NH_4^+ to form hydrazine (N_2H_4) which is further oxidized to N_2 (Hu et al., 2019). More commonly, NO is reduced to N_2O because the NO/N_2O couple has a highly positive reduction potential ($E^{\circ'}$ = +1.355 V) that enables its coupling with many half reactions (i.e., those with reduction potentials less than +1.355 V) to give positive overall voltages (Ducluzeau et al., 2014). Documented examples include N_2O production coupled to: abiotic oxidation of Fe(II) to Fe(III) (Onley et al., 2018; Stanton et al., 2018); autotrophic oxidation of sulfide to sulfur and of sulfur to sulfate (Liu et al., 2016); and heterotrophic oxidation of dissolved organics, such as acetate, or stored polyhydroxyalkanoates (PHAs), to CO_2 (Schalk-Otte, 2000; Meyer et al., 2005). N_2O accumulates in the atmosphere when its rate of production and emission exceeds its rate of removal (Stanton et al., 2018).

Others have noted that during the Great Oxygenation Event, rates of consumption and production of NO and N_2O likely responded to changes in *Cyanobacteria*-generated O_2, which would have enabled oxidation of NH_4^+ to NH_2OH and its further oxidation to NO_2^- (Schreiber et al., 2012) and NO (Schreiber et al., 2012; Caranto and Lancaster, 2017). Blockage of NOR by molecular oxygen may have provoked intracellular accumulation of NO to toxic levels, stimulating pathogen-host adaptation and co-evolution (Philippot, 2002; Lewis et al., 2015; Santana et al., 2017), paving the way for adoption of NO as a signaling molecule in microbial biofilms, plants, and animals (Moroz and Kohn, 2011; Arora et al., 2015; Santana et al., 2017).

Mass balances that seek to quantify sources of atmospheric N_2O emissions rely upon its monitoring in diverse environments, such as soils, estuaries, and bioreactors (Hu et al., 2015; Kuypers et al., 2018). Identification and classification of N_2O sources can be challenging due to the number and variety of N_2O-producing enzyme systems (Philippot, 2002; Zumft, 2005), including bacterial and archaeal NORs such as quinol-dependent nitric oxide reductase (qNOR), cytochrome-dependent nitric oxide reductase (cNOR), Cu_ANOR (Al-Attar and de Vries, 2015), sNOR (Stein et al., 2013; Ishii et al., 2014), NORvw (Hu et al., 2019), and hybrid cluster proteins (Zumft, 2005; Kahle et al., 2018) as well as fungal cytochrome P-450nor (Higgins et al., 2016). Tools are needed to discriminate among NORs and enable estimates of their contributions to N_2O emissions in dissimilar settings.

For this work, we focus on qNOR and cNOR because of their relatedness and ubiquity in natural and engineered systems. qNOR is electrogenic and has a proton channel that extends from the active site to the cytoplasm (Matsumoto et al., 2012; Jamali et al., 2020). By contrast, cNOR is not electrogenic (Blomberg and Siegbahn, 2013) and is reduced by a periplasmic cytochrome, such as cytochrome c_{551} (Matsumoto et al., 2012). Both enzymes play important roles in wastewater treatment bioreactors designed to remove total nitrogen from the effluent and to minimize N_2O emissions. Both enzyme types also play a role in "short-cut" N removal in CANDO (Coupled Aerobic-anoxic Nitrous Decomposition Operation), a process in which ammonia is converted to nitrite then sequentially reduced to NO then N_2O for energy production (Scherson et al., 2013; 2014; Myung et al., 2015; Gao et al., 2017; Weißbach et al., 2018; Wang et al., 2020). The energy production step can be achieved catalytically by decomposing N_2O to N_2 plus O_2, with release of 82 kJ/mol N_2O, or by combustion with CH_4 as fuel and N_2O as oxidant, generating 1219 kJ/mol CH_4, compared to 890 kJ/mol when O_2 is the CH_4 oxidant (Scherson and Criddle, 2014; Zhuge et al., 2020).

We include in this analysis nitric oxide dismutase (NOD) because the nucleotide sequence for *nod* is closely related to that of *qnor* and is present in *Candidatus Methylomirabilis oxyfera*, a strain that catalyzes the reaction $2NO \rightarrow N_2 + O_2$ (Ettwig et al., 2010, 2012; Zhu et al., 2017, 2019). O_2 derived from NOD is a substrate for methane monooxygenase (Ettwig et al., 2010) and likely has a similar role in alkane-oxidizing bacteria, including γ-*proteobacteria*, *Bacteriodetes*, *Firmicutes*, *Actinobacteria*, and *Chloroflexi* (Zhu et al., 2017, 2019; Hu et al., 2019). Additionally, *nod*-like genes present in the eukaryote *Foraminifera* were reported (Woehle et al., 2018).

The widespread distribution of *nor*/*nod* genes within Bacteria and Archaea, and even eukaryotes, suggests that variations in amino acid sequences preserve key functionalities, such as energy recovery or detoxification of NO, while enabling adaptation to specific environments, such as elevated temperature, high salinity, or low pH. To date, however, understanding of NOR phylogeny and diversity has been constrained to relatively few lineages. To address this deficiency, we carried out a comprehensive phylogenetic and functional analysis using whole genomes. The phylogenetic analysis revealed 9 clades within *qnor*/*nod* and 9 clades within *cnor*. By aligning amino acid sequences for q*nor* + *cnor*, *qnor*, and *cnor*, we identified four highly conserved regions for all NOR, including highly conserved histidine residues at the proposed active sites for qNOR and cNOR. We also

identified conserved sequences for primer design and microbiome analysis.

2 Materials and methods

2.1 Isolation and DNA extraction

Biomass samples collected from a laboratory-scale CANDO reactor on Day 0 and 90 (Scherson et al., 2014) were serially diluted, and aliquots of each dilution were spread on agar plates with nutrient broth (NB) media (RPI, Mt. Prospect, IL, USA). After incubation at 30 °C for two days, individual colonies on the plates were transferred to fresh NB agar plates. Purified colonies were cultivated at 30 °C on NB agar and maintained in a 20% glycerol stock at −80 °C. Samples of *Nocardioides daeguensis* 2C1-5 (KCTC 19772) and *Pseudomonas stutzeri* KC (DSM 7136) were obtained from Korean Collection for Type Cultures (KCTC) and Deutsche Sammlung von Mikroorganismen und Zellkulturen (DSMZ), respectively. For DNA extraction, all strains were aerobically cultivated in 100 mL liquid NB media at 30 °C for two days. Genomic DNA (gDNA) was extracted using MoBio UltraClean Microbial DNA Isolation Kit (MoBio, Carlsbad, CA, USA) per manufacturer's instructions.

2.2 Genome sequencing of isolated strains and data processing

Three isolates (*Comamonas* sp. CD01, *Alicycliphilus* sp. CD02, *Castellaniella* sp. CD04) were selected for whole genome sequencing. The genomes of *Comamonas* sp. CD01 and *Castellaniella* sp. CD04 were sequenced on an Illumina Hiseq 2500 platform (Elim Biopharmaceuticals, Inc., Hayward, CA, USA), and the genome of *Alicycliphilus* sp. CD02 was sequenced on an Illumina Hiseq 3000 platform (Clinical Genomics Center at Oklahoma Medical Research Foundation, Oklahoma City, OK, USA). Libraries were prepared using standard Illumina library preparation protocol. Quality measurements of raw reads were performed using fastqc (Andrews, 2010). Reads were quality-filtered with Trimmomatic 0.36. Three bases were trimmed from the leading and trailing ends of reads from both single-end and paired-end data sets. Quality thresholds of 15 and 20 were set for single-end and paired-end reads, respectively. Minimum sequence lengths required were 28 bases for single-end and 36 for paired-end reads. Quality filtered reads were assembled using SPAdes 3.10.0 (Bankevich et al., 2012). The paired-end reads were assembled with the –sc option. Kmer sizes of 21, 23, 25, 27, 29, 31, 33, 35, 37, 39, and 41 were used for shorter single-end reads, and kmer sizes of 21, 25, 29, 33, 337, 41, 45, 49, 53, 57, 61, 65, 69, 73, 77, 81, 89, 91, 95, 99 were used for paired-end data. Contaminant screening and genome completeness calculations were performed using CheckM (Parks et al., 2015). Open reading frame (ORF) calling was performed using Prokka with the metagenome flag to catch incomplete CDS at the ends of contigs (Seemann, 2014). Rapid Annotations using Subsystem Technology (RAST) was used for annotation using the contig and ORF data for each assembly (Aziz et al., 2008; Overbeek et al., 2014).

2.3 Alignment, primer design and phylogenetic tree construction

Near full-length nucleotide *qnor* (～2000 bp) and *cnorB* (～1200 bp) sequences from isolates and their close sequences were collected from the GenBank database (unless specified otherwise) and aligned using CLUSTAL_X (Thompson et al., 1997) then trimmed in Geneious (Kearse et al., 2012). Primer sets were designed based on the conserved regions in the aligned *qnor* and *cnorB* sequences. A *Comamonadaceae*-specific primer was designed based on the conserved regions found only in *Comamonadaceae*. Degeneracies were added to wobble positions. The phylogenetic tree of *qnor* and *cnorB* was reconstructed using the maximum likelihood method with bootstrap values based on 1000 replications in the MEGA7 program (Kumar et al., 2016).

2.4 Assignment of the nucleotide alignments to the qNOR and cNOR structures

Crystal structures of qNOR and cNOR were obtained from protein data bank (PDB) and modified through PyMOL Molecular Graphics System System (Schrödinger, LLC, NY, USA) (top two panels in Fig. 1) and BioRender© (bottom two panels in Fig. 1 and magnified amino acid figures in Figs. 2 and 3). The qNOR and cNOR structures were adapted from *Neisseria meningitidis* alpha14 (6L1X) (Jamali et al., 2020) and *Pseudomonas aeruginosa* PAO1 (5GUW) (Terasaka et al., 2017). Assignments for α-helices, β-sheets and transmembrane domains in the alignments were done according to Matsumoto et al. (2012) based on *Neisseria meningitidis* for the *qnor* + *cnor* alignment and the *qnor* alignment, with *Pseudomonas aeruginosa* for the *cnor* alignment.

2.5 PCR amplification

To detect *nor* genes with the designed primer sets, a polymerase chain reaction (PCR) was performed with 25 μL of a PCR mixture containing: 1.5 μM of forward and reverse primers, 2X Fail-Safe PCR buffer F (Epicenter, Madison, WI, USA), 2.5 units of AmpliTaq LD Taq Polymerase (Applied Biosystems, Foster City, CA, USA), and 50–80 ng of genomic DNA template. PCR thermocycling steps were carried out in a total of 40 cycles:

1) 95 °C for 5 min; 2) 10 initial cycles at 95 °C for 30 s, touch down from 59 °C to 54.5 °C with 0.5 °C gradient for 30 s, and 72 °C for 45 s, and an additional 30 cycles at 95 °C for 30 s, 57.5 °C for 30 s, 72 °C for 45 s, and 3) an extension at 72 °C for 10 min. The PCR product was verified by 1.5% agarose gel electrophoresis.

2.6 Data availability

Whole genomes for three isolated N_2O-producing strains were deposited to GenBank under accession numbers of ASM289430v1, ASM289435v1, and ASM289431v1 for *Comamonas* sp. CD01, *Alicycliphilus* sp. CD02 and *Castellaniella* sp. CD04, respectively.

3 Results

3.1 Conserved nucleotides/amino acids and NOR diversity

Figure 1 illustrates the crystal structures of qNOR (Jamali et al., 2020) and cNOR (Terasaka et al., 2017), with the highlighted conserved amino acids. These features were used to design *nor*-universal primers and *qnor*- or *cnor*-universal primers. The most conserved amino acids are adjacent to the active site of qNOR or cNOR and contrast with the high diversity of non-conserved regions (Figs. S1 and S2).

Alignments of qNOR and cNOR amino acid sequences were used to identify conserved regions for primer design or for metagenome analysis, including universally conserved regions, regions specific to *qnor* and *cnor*, and regions specific to *Comamonadaceae*. Universally conserved sequences for *qnor* and *cnor* are located at base pairs 249–271, 1666–1688, 2069–2091, and 2152–2174 of the *qnor* + *cnor* alignment (Fig. 2). As shown in Table 1, at least two amino acids are conserved within each conserved region across all 548 *nor* sequences. Because regions encoding conserved amino acid sequences were found for all *qnor* (*nod*) and *cnor*, primer design required degeneracy at wobble positions. The first conserved region is located at nucleotides 249–271 between α1 and α2, where two Gs are 100% conserved, and a second G and Y encode residues for calcium ligands (Matsumoto et al., 2012). A forward universal primer for *qnor* + *cnor* (qcU1F) was designed for this region. The second conserved region 1666–1688 is located in TM VIII (TM VI of cNOR), where H and E are 100% conserved. In TM VIII, H binds metal ligands, and E is one of the residues lining a water channel that leads to the cytoplasm (Matsumoto et al., 2012). The third and fourth conserved regions, 2069–2091 and 2152–2174, are located in TM XI and TM XII (TM IX and TM X of cNOR), respectively. Two Gs in 2069–2091 and two Hs in

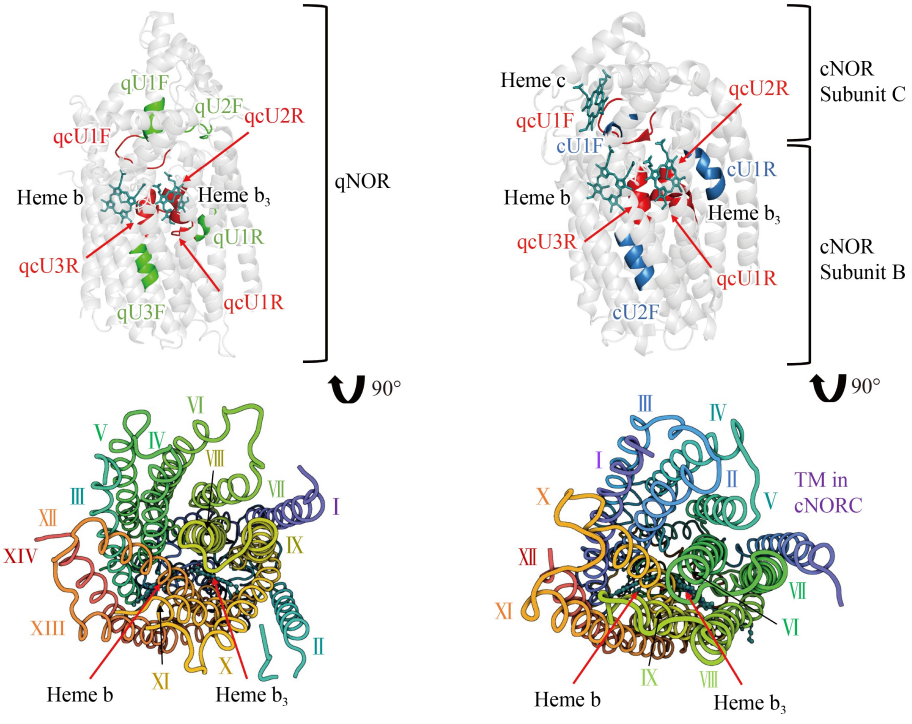

Fig. 1 Crystal structures of qNOR (left) from *Neisseria meningitidis* alpha14 (6L1X) and cNOR (right) from *Pseudomonas aeruginosa* PAO1 (5GUW). The top two panels show profile views of NOR with a top segment located within the periplasmic space and alpha helices spanning the cytoplasmic membrane and extending into the cytoplasm. Primers in this study for *qnor* and *cnor* universal (qcU), *qnor*-universal (qU), and *cnor*-universal (cU) based on the conserved amino acids are shown in red, green and blue, respectively. The bottom two panels show views looking up into the transmembrane helices from inside the cytoplasm. Roman numerals indicate transmembrane domains.

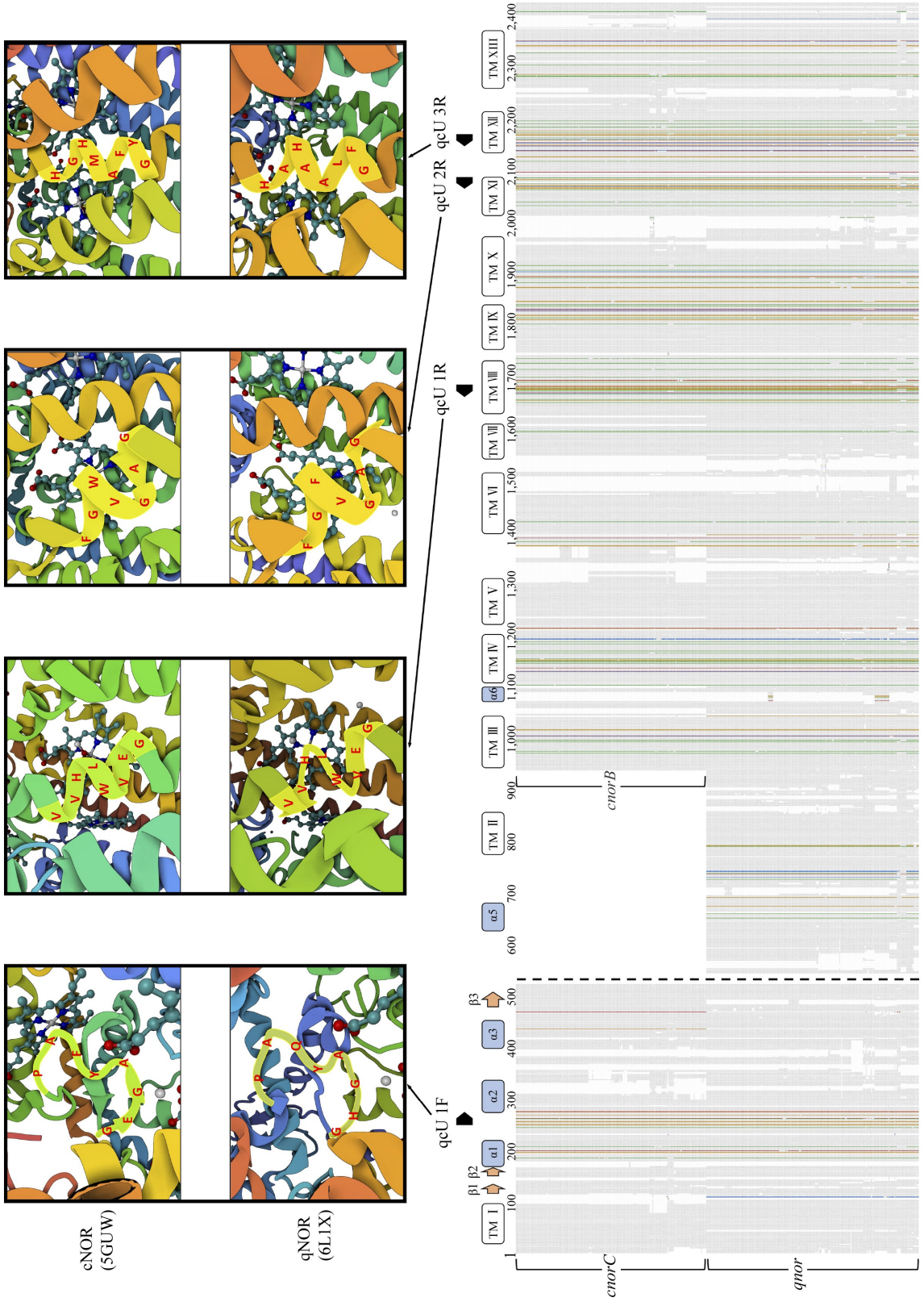

Fig. 2 *qnor* + *cnorC* and *qnor* + *cnorB* nucleotide sequence alignments. The colored nucleotide positions represent 95% conserved nucleotides across all 548 *qnor* + *cnor* sequences (Red: A, Yellow: G, Green: T, Blue: C). α-helices and β-sheets are indicated with blue boxes and orange arrows, respectively. The α4 helix between alignments for *cnorC* + *qnor* and *cnorB* + *qnor* was omitted, and TM XIV (i.e., TM XII of cNOR) at the end of the sequence are not shown.

Table 1 Conserved amino acids and primer sets for *qnor* + *cnor* (*nor*-universal, qcU) designed in this study

Primer name	Primer direction	Primer sequence (5'−3')	Amino acid number	Nucleotide sequence (5'−3')	Amino acid type	Amino acid (%)
qcU 1F	Forward	GGNVANGGNDSN TAYBWNGSNCC	1	GGN	G	100
			2	VAN	E	40.3
					H	40.1
					N	10.0
			3	GGN	G	100
			4	DSN	A	75.4
					S	15.1
			5	TAY	Y	95.3
			6	BWN	F	32.5
					Q	18.6
					Y	18.1
					L	12.0
					V	10.4
			7	GSN	A	78.1
					G	20.4
			8	CC	P	91.8
qcU 1R	Reverse	CCYTCNACCCAN ARRTGNAYNAY	1	RTN	V	77.6
					I	10.9
			2	RTN	V	80.3
					I	19.7
			3	CAY	H	100
			4	YTN	L	88.1
			5	TGG	W	97.6
			6	GTN	V	99.3
			7	GAR	E	100
			8	GG	G	83.2
qcU 2R	Reverse	RAANCCNMRNA VNCCNGCNCC	1	GGN	G	100
			2	GCN	A	98.4
			3	GGN	G	97.4
			4	BTN	V	69.3
					L	16.2
			5	YKN	W	38.1
					F	34.3
					L	24.3
			6	GGN	G	100
			7	TTY	F	87.8
qcU 3R	Reverse	CCVWWNADNGCN RNRTGNSCRTG	1	CAY	H	100
			2	GSN	G	50.5
					A	33.0
			3	CAY	H	100
			4	NYN	A	37.8
					L	32.7
					M	11.3
			5	GCN	A	94.7

(*Continued*)

Primer name	Primer direction	Primer sequence (5'−3')	Amino acid number	Nucleotide sequence (5'−3')	Amino acid type	Amino acid (%)
			6	HTN	F	50.4
					L	37.6
					M	11.3
			7	WWB	F	53.5
					Y	26.1
					M	11.9
			8	GG	G	97.4

Note: Degeneracies were added to wobble positions as per the IUPAC code: R = A or G; Y = C or T; S = G or C; W = A or T; K = G or T; M = A or C; B = C, G or T; D = A, G or T; H = A, C or T; V = A, C or G; N = A, T, C or G. Key for amino acids: A = alanine, R = arginine, N = asparagine, D = aspartate, C = cysteine, Q = glutamine, E = glutamate, G = glycine, H = histidine, I = isoleucine, L = leucine, K = lysine, M = methionine, F = phenylalanine, P = proline, S = serine, T = threonine, W = tryptophan, Y = tyrosine, V = valine.

2152–2174 are 100% conserved. The two Hs in TM XII are known residues for metal ligands (Matsumoto et al., 2012). For the second, third, and fourth conserved regions, reverse universal primers (qcU1R, qcU2R, qcU3R) were designed to capture highly variable regions, which can be used with the Clade-specific forward primers. Because *cnorC* and *cnorB* genes are co-located in all genomes, two primers, one for *cnorC* and one other for *cnorB*, can detect the targeted *cnor* fragments.

Conserved nucleotide regions in *cnor* are located at base pairs 213–232 in the *cnorC* alignment, at base pairs 187–204 and 757–777 in the *cnorB* alignment. These three conserved regions are located between α1 and α2, at TM II, and at TM VII of the cNOR enzyme (light green), respectively (Fig. 3). Conserved nucleotide regions in the *qnor* alignment are present at base pairs 251–270, 731–750, 1158–1175, and 1887–1909. These four conserved regions are located in α2 of the N-terminal region, between α2 and TM II, at TM IV, and at TM X of the qNOR enzyme (light green), respectively (Fig. 3). Tables S1 and S2 summarize the conserved amino acids and corresponding primers based on alignments of *cnor* and *qnor*. As shown in the *qnor* alignment (Fig. 3), members of the family *Comamonadaceae* were enriched in bench-scale CANDO bioreactor communities (*Comamonas* and *Alicycliphilus*) (Scherson et al., 2013, 2014) and in a pilot-scale reactor community (*Diaphorobacter*) (Wang et al., 2020). Bioreactor isolates *Comamonas* sp. CD01 and *Alicycliphilus* sp. CD02 have unique *Comamonadaceaea* sequences (Coma-specific 1 and 2), marked with orange brackets in the *qnor* Clade 1 alignment (Fig. 3). Compared to the closely related *qnor* genes, five additional amino acids and one or two amino acids are found in Coma-specific sections 1 and 2, respectively (Fig. S1). A *Comamonadaceae*-specific reverse primer (qSComa1R) was designed (Table S3) based on Coma-specific section 2 (Table S4), which can be used with Clade-specific forward primers. As shown in Fig. S3, two *nod*-like sequences (one gene and one transcript) from a eukaryotic cell of *Foraminifera* are located directly adjacent to two *nod* genes from *Candidatus Methylomirabilis oxyfera* (DAMO2434 and DAMO2437). We therefore designed specific primers to detect *nod* (Table S5).

3.2 Phylogenetic tree construction for *nor* and *nod*

Figure 4 illustrates phylogenetic relationships for 289 *qnor/nod* and 259 *cnorB* sequences from databases, with five from sequenced genomes of three isolates from CANDO bioreactors (flagged with red dots in Fig. 4). These five *nor* were detected in three CANDO bioreactor isolates: *Comamonas* sp. CD01 and *Alicycliphilus* sp. CD02 had one *qnor*, and *Castellaniella* sp. CD04 had two *qnor* and one *cnor*. Figure 4 also includes two *nod* genes (DAMO2434 and DAMO2437) in *qnor* Clade VI from *Candidatus Methylomirabilis oxyfera* in candidate division NC10. These genes are flagged with green dots in Figs. 4 and S3.

Phylogenetic analysis of *qnor* revealed nine clades: (I–II) *Proteobacteria* (α, β, χ); (III) *Planctomycetes* & *Acidobacteria*; (IV) *Cyanobacteria*; (V) *Actinobacteria*; (VI) *Bacteriodetes*; (VII) *Euryarchaeota*; (VIII) *Crenarchaeota*; and (IX) *Firmicutes* & *Aquificae*. It also revealed nine *cnorB* clades: (I–IV) *Proteobacteria* (α, β, χ, ε, ζ); (V) *Deinococcus-Thermus*; (VI–VIII) *Proteobacteria* (α, β, χ, δ, *Oligoflexia*); and (IX) *Bacteriodetes*. Greatest diversity was observed in the q*nor/nod* lineages, where there is evidence of gene duplication and/or horizontal gene transfer. Of the 289 *qnor* genes, 47 (16.3%) are present with another *qnor* within the same strains. Of the 259 *cnor* genes, 22 (8.5%) are present with another *cnor* within the same strains. Of the 548 *nor* genes, 60 (10.9%) are present in the same strains which have both *qnor* and *cnor*, as in *Castellaniella* sp. CD04. In total, of the 478 microorganisms for 548 *nor*, 64 (13.4%) have more than one copy of *nor*. When two or more copies of *nor* were present within a single strain, their locations in the sequenced genomes were specified (Figs. S3 and S4).

3.3 Primer testing

Table 2 summarizes data demonstrating the selectivity of

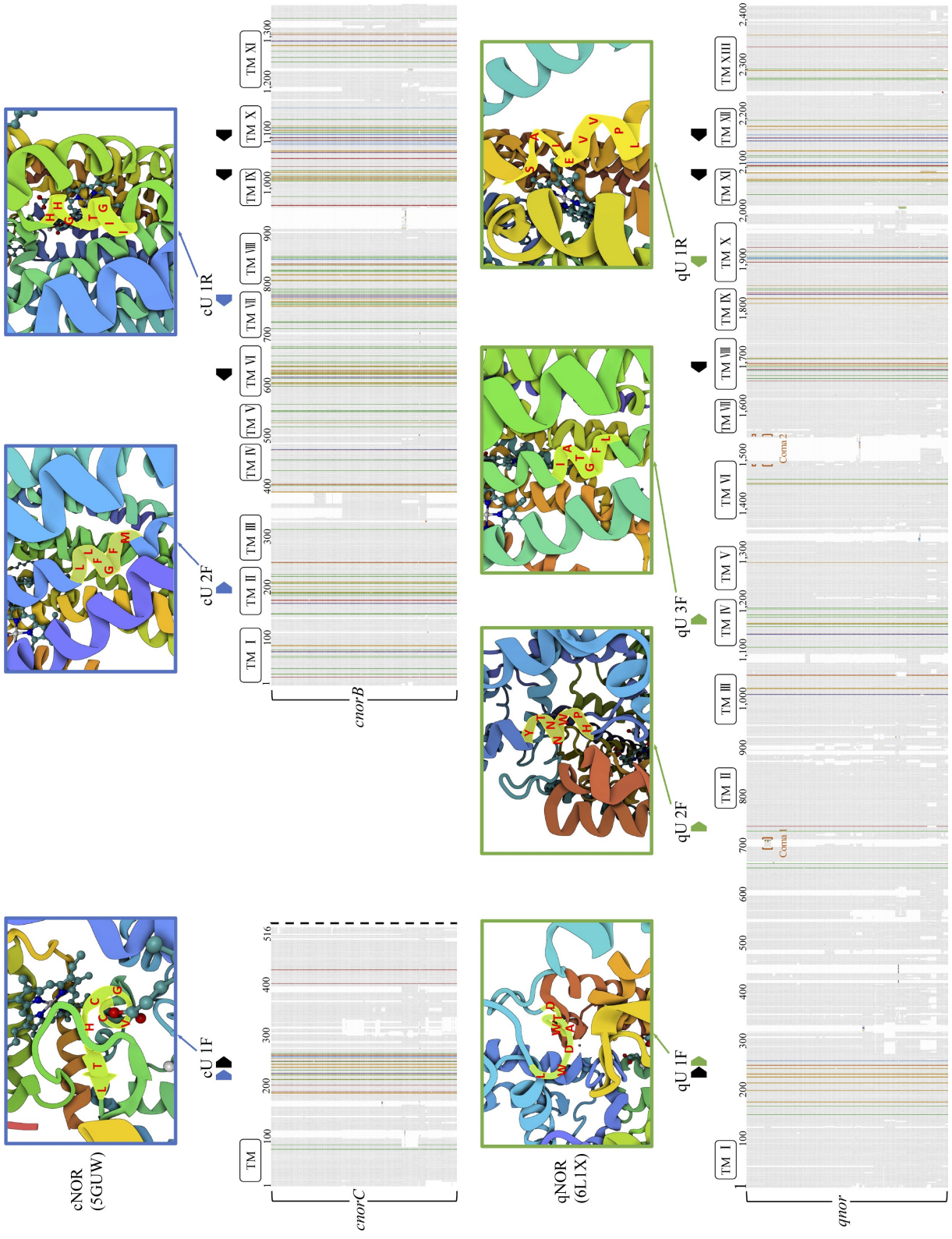

Fig. 3 *qnor* and *cnor* nucleotide sequence alignments. The colored nucleotide positions represent 99% conserved nucleotides across all 289 *qnor* or 259 *cnor* sequences (Red: A, Yellow: G, Green: T, Blue: C).

newly designed primers for pure cultures containing *qnor* or *cnor*, and include a negative control, *Nocardioides daeguensis* 2C1-5 (Cui et al., 2013). This strain does not have *nor* or *nod* in its sequenced genome (GenBank database ASM1919296v1). All of the *nor*-universal and *qnor* or *cnor*-universal primers designed in this study

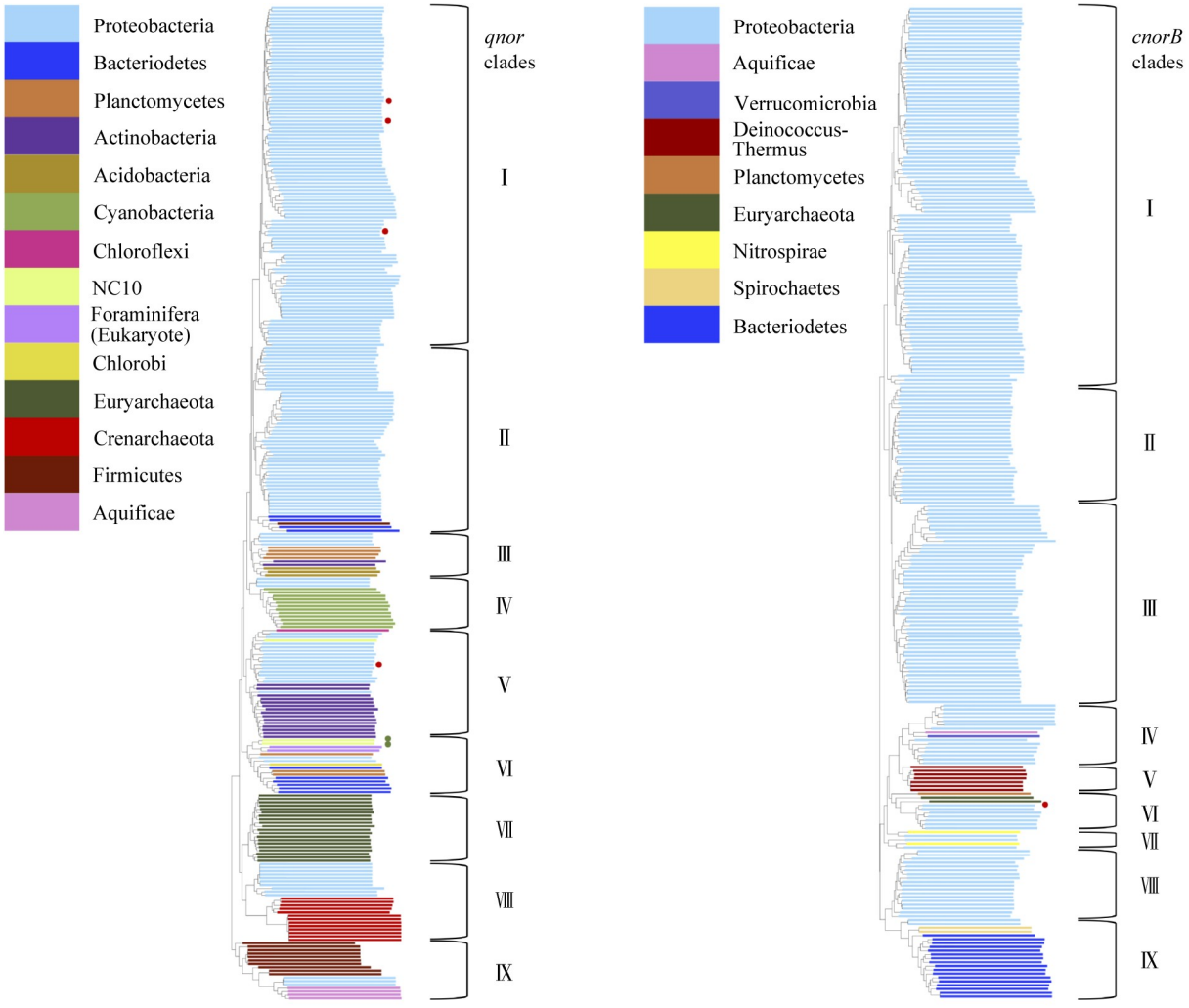

Fig. 4 Evolutionary relationship of 289 *qnor* and 259 *cnorB* using the maximum likelihood method. Four *qnor* sequences and one *cnor* sequence (marked with red dots) are from the sequenced genomes of N_2O-producing bioreactor isolates. All other sequences were obtained from databases.

enabled amplification of the expected nucleotide sequences when combined with appropriate Clade-specific primers. Primer dimerization resulted when both forward and reverse *nor*-universal primers were used together or when one *nor*-universal primer and one *qnor*- or *cnor*-universal primer were used together. This outcome was attributed to wobble positions. Accordingly, we designed specific primers based on *qnor* or *cnor* of a single strain and were able to detect Clade-wide *qnor* or *cnor* genes by allowing a few mismatches for amplification. Three to four times higher concentrations of primers were used in primer testing because wobble positions can be occupied at a probability of 1/n (where *n* = number of nucleotides in a given location, i.e. 1, 2, 3 or 4). We then introduced Clade-specific primer examples designed to match locations within *qnor*- or *cnor*-universal primers (Tables S6 and S7). These specific primers can be used with *nor*-universal, *qnor*-universal, and *cnor*-universal primers. Due to their universality, however, some results showed more than one amplified sequence (Fig. S5). The target gene in multiple bands can be recovered by gel purification steps to analyze amplified sequences in downstream work. For the negative control, none of the newly designed primers amplified *qnor* or *cnor* genes for the target fragments, as expected.

4 Discussion

4.1 Production of N_2O in engineered systems

Enrichment of N_2O-producing populations from ammonia-rich anaerobic digestate has been achieved in two steps: in the first, ammonia is aerobically oxidized to nitrite; in the second, an electron donor, such as acetate, is added under anaerobic conditions to induce synthesis of intracellular PHA storage granules. The nitrite-rich effluent from the aerobic bioreactor is fed to PHA-rich cells enabling coupled oxidation of PHA and reduction of nitrite to N_2O

Table 2 Application of newly designed *nor*-universal (qcU), *qnor* and *cnor* Clade-specific (based on *qnor*-universal (qU) and *cnor*-universal (cU) primers), and *Comamonadaceae*-specific (qSComa1R) primer sets to pure strains

Pure strains	Primer sets	Results
Comamonadaceae (*qnor* Clade I) * *Comamonas* sp. CD01 ** *Alicycliphilus* sp. CD02	qU2F (*qnor* Clade I) qcU1R (*nor*-universal)	* +
	qU2F (*qnor* Clade I) qcU3R (*nor*-universal)	* +
	qU2F (*qnor* Clade I) qSComa1R (family-specific)	** +
Castellaniella sp. CD04 (*qnor* Clade V)	qU2F (*qnor* Clade V) qcU1R (*nor*-universal)	+
	qU2F (*qnor* Clade V) qcU2R (*nor*-universal)	+
	qU1R (*qnor* Clade V) qcU1F (*nor*-universal)	+
Castellaniella sp. CD04 (*cnor* Clade VI)	cU2F (c*nor* Clade VI) qcU1R (*nor*-universal)	+
	cU2F (c*nor* Clade VI) qcU2R (*nor*-universal)	+
	cU1R (c*nor* Clade VI) qcU1F (*nor*-universal)	+
Pseudomonas stutzeri KC (*cnor* Clade III)	cU2F (c*nor* Clade III) qcU1R (*nor*-universal)	+
	cU2F (c*nor* Clade III) qcU2R (*nor*-universal)	+
	cU1R (c*nor* Clade III) qcU1F (*nor*-universal)	+
Nocardioides daeguensis 2C1-5 (Negative Control)	qU2F (*qnor* Clade I) qcU1R (*nor*-universal)	–
	qU2F (*qnor* Clade I) qcU2R (*nor*-universal)	–
	qU2F (*qnor* Clade I) qcU3R (*nor*-universal)	–
	cU2F (c*nor* Clade III) qcU1R (*nor*-universal)	–
	cU2F (c*nor* Clade III) qcU2R (*nor*-universal)	–
	cU1R (c*nor* Clade III) qcU1F (*nor*-universal)	–

Note: *Nocardioides daeguensis* 2C1-5 (Cui et al., 2013) was used as a negative control. "+" and "–" represent presence or absence of the amplification for the target fragments. Examples suggested for Clade-specific primers and detailed information on primer testing including a gel photo are provided in Table S6 , Table S7, and Fig. S5.

(Schalk-Otte, 2000; Meyer et al., 2005). This strategy was renamed the "decoupled strategy" because acetate addition to produce PHB is separated in time from the addition of nitrite (Scherson et al., 2013). The dominant microorganisms in the first laboratory-scale CANDO bioreactors were *Comamonas*, *Alicycliphilus*, and *Castellaniella* (Scherson et al., 2013, 2014). Isolation and whole genome sequencing of three isolates (*Comamonas* sp. CD01, *Alicycliphilus* sp. CD02, *Castellaniella* sp. CD04) revealed complete pathways for denitrification and PHA synthesis. All three species contained *qnor*. In a subsequent 300-day pilot-scale study, community structure varied greatly due to disturbances in upstream system operation (Wang et al., 2020). For days 160–260, qNOR-harboring *Diaphorobacter* were dominant, but on days 250–300 cNOR-harboring *Thauera* and *Paracoccus* became dominant. In follow-up bench-scale studies, optimized operational conditions selected for a *Defluviicoccus* strain (Wang et al., 2020). This strain was not isolated, but three *qnor* genes from two sequenced *Defluviicoccus* strains are present in Clade II of the *qnor* tree (Fig. S3). This is important because *Defluviicoccus* are glycogen-accumulating organisms (GAOs), and other GAOs, such as strains of *Competibacter* and *Contendobacter*, appear in Clade II of the *cnor* tree (Fig. S4).

In the CANDO + P process (Gao et al., 2017), phosphate-accumulating organisms (PAOs), are dominant, and the *qnor* of *Candidatus Accumulibacter phosphatis* UW-1 clade IIA (CP001715.1) appears in Clade II of the *qnor* tree (Fig. S3). Another CANDO strategy makes use of stable methane-fed batch reactors dominated by *Methylocystis*, α-proteobacterial methanotrophs (Myung et al., 2015). The genus *Methylocystis* appears in the *qnor* tree with two plasmid-encoded *qnor* genes from *Methylocystis* sp. SC2 in Clade II. Other *Methylocystis qnor* genes are present in Clade VIII.

It is generally held that qNOR evolved prior to cNOR and likely functions as the primary mediator of NO

reduction under extreme conditions, a conclusion consistent with the detection of qNOR in extremophiles. Hypersaline environments select for *Halomonas* in N_2O-producing bioreactors (Li et al., 2018), and operation at pH 4.5 selects for *Comamonas* and *Xanthomonas* (Zhuge et al., 2020). *Halomonas*, *Comamonas*, and *Xanthomonas* all appear in the *qnor* phylogenetic tree (Fig. S3).

As previously shown in the studies for deliberate N_2O production (Scherson et al., 2013, ; Myung et al., 2015; Gao et al., 2017; Li et al., 2018; Weißbach et al., 2018; Wang et al., 2020; Zhuge et al., 2020), engineered systems were dominated by highly variable microbial communities, which appeared in different clades of the phylogenetic trees (Fig. 4). Observing conserved amino acids for all *nor* and *nod*, where the *nor* universal primers were designed in this study, enables us to capture the diverse *nor*/*nod* genes in N_2O-producing engineered systems. Furthermore, the microbial communities and the accompanying *nor* types can shift within the same reactor, depending upon operational factors (Scherson et al., 2013, 2014; Wang et al., 2020; Zhuge et al., 2020). In such cases, the Clade-specific primers can target phylogenetic groups expected for specific operational conditions.

4.2 Evaluation and comparison of *nor*/*nod* primers

Prior work on primers for detection of *nor* has focused more on *cnor* than *qnor*. This is because *cnor* was the first *nor* detected and is abundant in engineered and natural systems. Earlier efforts targeted specific phylogenetic groups. Ma et al. (2019) reported that *qnor* primers developed by Braker and Tiedje (2003) were the only *qnor*-universal primer sets then available, but only enabled 43.2%–45.8% overall coverage, with higher coverage for *Proteobacteria* (> 50%) and poor coverage for other taxa such as *Actinobacteria*, *Firmicutes*, and *Archaea*. Primers developed by Braker and Tiedje (2003) for *qnor* and *cnor* were limited to *Proteobacteria* and *Cyanobacteria*; *qnor* primers developed by Verbaendert et al. (2014) were limited to *Firmicutes*; and *cnor* primers developed by Casciotti and Ward (2005) and Dandie et al. (2007) were limited to *Proteobacteria*. Because *qnor* primers developed by Verbaendert et al. (2014) were based upon primers for *Geobacillus* (*Firmicutes*), the overall coverage was low (4.6%). Primers developed for *cnor* by Braker and Tiedje (2003) and Casciotti and Ward (2005) achieved 70.7%–81.9% overall coverage with higher coverage for *Proteobacteria* (> 94%), but lower coverage for other taxa. Heylen et al. (2007) reported that only 30% of cultivated denitrifying bacteria yielded a *nor* amplicon with the *qnor* primers available at that time. Specific *cnorB* primers based on *Pseudomonas mandelii* by Dandie et al. (2007) had low coverage for overall taxa (⩽ 4%), as intended.

The availability of sequenced genomes facilitates primer design based upon alignment and comparison of conserved amino acid regions across many species. To maximize primer coverage, we focused on the most conserved amino acids in the qNOR and cNOR alignments. Of the four conserved regions within the alignment (Fig. 2), nucleotide region 1666–1688 is most conserved across all *nor* sequences, with four highly conserved residues (H: 100%, W: 97.6%, V: 99.3%, E: 100%) located in TM VIII (TM VI of cNOR). Braker and Tiedje (2003) used this region for design of qnorB5R primers and Casciotti and Ward (2005) used it for design of cnorB3 primers. The *nor*-universal reverse primers (qcU1R, qcU2R, qcU3R) in this study overlap with previously developed primers. The overlap includes as many as 17 and 9 base pairs in the case of qnorB5R and qnorB7R, 18 and 8 base pairs in the case of cnorB6R and cnorB7R, and 20 and 15 base pairs in the case of cnorB3 and cnorB6. qcU1R, qcU2R, and qcU3R are designed to detect both *qnor* and *cnor* (Table S8).

After identification of *nod* in *Candidatus Methylomirabilis oxyfera* (Ettwig et al., 2010,), several research groups screened for its presence in engineered and natural systems with specific primers (Zhu et al., 2017, 2019). Several of these primers were designed for a general *nod* based on DAMO2437 from *Candidatus Methylomirabilis oxyfera* (Zhu et al., 2017) and an NC10 *nod* (840F and 1012R) (Zhu et al., 2019). Unlike these general *nod* primers, the *nod*-specific primers developed in this study (Table S5) were designed using the same positions for *nor*-universal primers (qcU1F, qcU1R, qcU2R, qcU3R) but integrating *nod*-specific amplicons for data processing with *qnor* and *cnor* genes co-amplified with the *nor*-universal primers. No overlapping regions were observed for four *nor*-universal primers and general *nod* primers at seven different positions of DAMO2437, except the shared region between nod2015R and qcU3R which has 6 overlapping nucleotides (Table S8).

4.3 Evolution and phylogeny of *qnor* and *cnor*

Researchers have proposed that ancestral qNOR supported respiration with nitric oxide, and that cNOR evolved from qNOR, providing a structural basis for O_2 respiration during and after the Great Oxygenation Event (Matsumoto et al., 2012; Ducluzeau et al., 2014). The *nor* phylogenetic trees made possible with hundreds of whole genome sequences are consistent with this hypothesis and enable a more comprehensive view of *qnor* and *cnor* relatedness and evolution. Figure 4 gives an overview of the phylogenetic trees for both *qnor* and *cnor*. Detailed trees for all species included in this analysis are provided in Fig. S3, Fig. S4, Text S1, and Text S2.

In general, microorganisms that convert NO to N_2O are commonly reported as possessing either *qnor* or *cnor* but not both. In this study, however, multiple taxa were identified that contain both *qnor* and *cnor*. Examples

include *Castellaniella, Rhodanobacter, Acidovorax, Diaphorobacter, Melaminivora, Microbulbifer, Marinobacter, Aquiflexum, Halomonas, Methylomonas, Methylocaldum, Bdellovibrio*, *Flavobacteriaceae*, *Hahella*, *Vogesella*, *Undibacterium*, *Nitrosococcus, and Massilla*. Some *cnor* genes from these strains are present in deep-branching *cnor* clades (VI, VIII, and IX), suggesting acquisition by horizontal gene transfer.

Several microbial groups, including *Anaeromyxobacter*, *Castellaniella*, *Cupriavidus*, *Burkholderia*, *Herminiimonas*, *Pusillimonas*, *Sphingomonas*, *Defluviicoccus*, *Bacillus azotoformans*, *Candidatus Methylomirabilis oxyfera*, *Mycobacterium*, *Acaryochloris*, *Halopiger*, *Haloterrigena*, and *Methylocystis* contain multiple copies of *qnor*. Similarly, several microbial groups, including *Thiobacillus*, *Pseudomonas*, *Azoarcus*, *Azospirillum*, *Methylophaga*, *Sedimenticola*, *Sulfurimonas*, *Candidatus Sulfobium mesophilum* harbor multiple copies of *cnor*. Others have reported multiple copies of *nor* and other denitrifying genes within a single microorganism (Philippot, 2002; Chain et al., 2006).

The present study demonstrates that sequence similarities between multiple copies of *qnor* or *cnor* within a single strain are typically low. *Anaeromyxobacter dehalogenans* 2CP-C, for example, harbors three copies of *qnor* in Clades III, IV, and V. *Anaeromyxobacter* contains nitrous oxide reductase (*nosZ*), but has been classified as a non-denitrifying N_2 producer (Shan et al., 2021) because it lacks nitrite reductase (*nirS* or *nirK*) (Onley et al., 2018). The fact that *Anaeromyxobacter* possesses multiple copies of *nor* suggests modular expression of *nor*, perhaps linked to community structure (Graf et al., 2014). Numerous *Burkholderia* strains have two copies of *qnor* in Clade II and VIII, and multiple *Pseudomonas* strains harbor two copies of *cnor* in Clade III and VI (Figs. S3 and S4). These features suggest adaptation to different environments enabled by horizontal gene transfer (Chain et al., 2006). On the other hand, some strains have similar copies of *qnor* (*Methylocystis* sp. SC2) or *cnor* (*Sedimenticola thiotaurini* SIP-G1), perhaps the result of gene duplication.

5 Conclusions

For this work, *nor* genes in diverse microbial groups and some Eukarya were incorporated into the *qnor* (*nod*) and *cnor* phylogenetic trees using representative *qnor* (*nod*) and *cnor* sequences. Despite the diversity of nucleotides/amino acids sequences, most conserved regions were identified in the *qnor* + *cnor*, *qnor*, and *cnor* alignments. Primer sets designed to detect both *qnor* and *cnor* (*nor*-universal), *qnor* (*qnor*-universal), and *cnor* (*cnor*-universal) enabled amplification of *qnor* and *cnor* genes from pure strains, including isolates from N_2O-producing bioreactors, when combined with Clade-specific primers. Moreover, *nod*-specific primers enabled detection of *nod* genes with the same length of fragments amplified by *nor*-universal primers for all *qnor*, *cnor*, and *nod*. *Comamonadaceae* family-specific primers selectively detected *qnor* in the *Comamonadaceae* family. This work opens the door for more detailed analysis of environmental drivers of NOR function, structure, and phylogeny and will inform strategies for management of N_2O production in diverse environments.

Acknowledgements This research was supported in part by a grant from the US National Science Foundation Engineering Research Center Reinventing the Nation's Urban Water Infrastructure (ReNUWIt) (Award No. EEC-1028968) and in part by a grant from the NASA Center (USA) for the Utilization of Biological Engineering in Space (CUBES) (Award No. NNX17AJ31G). We thank Dr. Jizhong Zhou and the Institute of Environmental Genomics at the University of Oklahoma, Norman (OK, USA), for sequencing of *Alicycliphilus* sp. CD02.

Competing Interests The authors declare no conflict of interests.

Electronic Supplementary Material Supplementary material is available in the online version of this article at https://doi.org/10.1007/s11783-022-1562-3 and is accessible for authorized users.

References

Al-Attar S, de Vries S (2015). An electrogenic nitric oxide reductase. FEBS Letters, 589(16): 2050–2057

Andrews S (2010). FastQC: A quality control tool for high throughput sequence data (Babraham Bioinformatics). Cambridge, England: Babraham Institute

Arora D P, Hossain S, Xu Y, Boon E M (2015). Nitric oxide regulation of bacterial biofilms. Biochemistry, 54(24): 3717–3728

Aziz R K, Bartels D, Best A A, DeJongh M, Disz T, Edwards R A, Formsma K, Gerdes S, Glass E M, Kubal M, Meyer F, Olsen G J, Olson R, Osterman A L, Overbeek R A, McNeil L K, Paarmann D, Paczian T, Parrello B, Pusch G D, Reich C, Stevens R, Vassieva O, Vonstein V, Wilke A, Zagnitko O (2008). The RAST server: rapid annotations using subsystems technology. BMC Genomics, 9(1): 75

Bankevich A, Nurk S, Antipov D, Gurevich A A, Dvorkin M, Kulikov A S, Lesin V M, Nikolenko S I, Pham S, Prjibelski A D, Pyshkin A V, Sirotkin A V, Vyahhi N, Tesler G, Alekseyev M A, Pevzner P A (2012). SPAdes: A new genome assembly algorithm and its applications to single-cell sequencing. Journal of Computational Biology, 19(5): 455–477

Blomberg M R A, Siegbahn P E M (2013). Why is the reduction of NO in cytochrome c dependent nitric oxide reductase (cNOR) not electrogenic? Biochimica et Biophysica Acta (BBA) Bioenergetics, 1827(7): 826–833

Braker G, Tiedje J M (2003). Nitric oxide reductase (*norB*) genes from pure cultures and environmental samples. Applied and Environmental Microbiology, 69(6): 3476–3483

Caranto J D, Lancaster K M (2017). Nitric oxide is an obligate bacterial nitrification intermediate produced by hydroxylamine oxidoreductase. Proceedings of the National Academy of Sciences

of the United States of America, 114(31): 8217–8222

Casciotti K L, Ward B B (2005). Phylogenetic analysis of nitric oxide reductase gene homologues from aerobic ammonia-oxidizing bacteria. FEMS Microbiology Ecology, 52(2): 197–205

Chain P S G, Denef V J, Konstantinidis K T, Vergez L M, Agullo L, Reyes V L, Hauser L, Cordova M, Gomez L, Gonzalez M, Land M, Lao V, Larimer F, LiPuma J J, Mahenthiralingam E, Malfatti S A, Marx C J, Parnell J J, Ramette A, Richardson P, Seeger M, Smith D, Spilker T, Sul W J, Tsoi T V, Ulrich L E, Zhulin I B, Tiedje J M (2006). *Burkholderia xenovorans* LB400 harbors a multi-replicon, 9. 73-Mbp genome shaped for versatility. Proceedings of the National Academy of Sciences, 103(42): 15280–15287

Cui Y, Woo S G, Lee J, Sinha S, Kang M S, Jin L, Kim K K, Park J, Lee M, Lee S T (2013). *Nocardioides daeguensis* sp. nov., a nitrate-reducing bacterium isolated from activated sludge of an industrial wastewater treatment plant. International Journal of Systematic and Evolutionary Microbiology, 63(10): 3727–3732

Dandie C E, Miller M N, Burton D L, Zebarth B J, Trevors J T, Goyer C (2007). Nitric oxide reductase-targeted real-time PCR quantification of denitrifier populations in soil. Applied and Environmental Microbiology, 73(13): 4250–4258

Ducluzeau A L, Schoepp-Cothenet B, van Lis R, Baymann F, Russell M J, Nitschke W (2014). The evolution of respiratory O_2/NO reductases: An out-of-the-phylogenetic-box perspective. Journal of the Royal Society, Interface, 11(98): 20140196

Ettwig K F, Butler M K, Le Paslier D, Pelletier E, Mangenot S, Kuypers M M M, Schreiber F, Dutilh B E, Zedelius J, de Beer D, Gloerich J, Wessels H J C T, van Alen T, Luesken F, Wu M L, van de Pas-Schoonen K T, Op den Camp H J M, Janssen-Megens E M, Francoijs K J, Stunnenberg H, Weissenbach J, Jetten M S M, Strous M (2010). Nitrite-driven anaerobic methane oxidation by oxygenic bacteria. Nature, 464(7288): 543–548

Ettwig K F, Speth D R, Reimann J, Wu M L, Jetten M S M, Keltjens J T (2012). Bacterial oxygen production in the dark. Frontiers in Microbiology, 3: 273

Fowler D, Coyle M, Skiba U, Sutton M A, Cape J N, Reis S, Sheppard L J, Jenkins A, Grizzetti B, Galloway J N, Vitousek P, Leach A, Bouwman A F, Butterbach-Bahl K, Dentener F, Stevenson D, Amann M, Voss M (2013). The global nitrogen cycle in the twenty-first century. Philosophical Transactions of the Royal Society of London. Series B, Biological Sciences, 368: 20130164

Gao H, Liu M, Griffin J S, Xu L, Xiang D, Scherson Y D, Liu W T, Wells G F (2017). Complete nutrient removal coupled to nitrous oxide production as a bioenergy source by denitrifying polyphosphate-accumulating organisms. Environmental Science & Technology, 51(8): 4531–4540

Graf D R H, Jones C M, Hallin S (2014). Intergenomic comparisons highlight modularity of the denitrification pathway and underpin the importance of community structure for N_2O emissions. PLoS One, 9(12): e114118

Heylen K, Vanparys B, Gevers D, Wittebolle L, Boon N, De Vos P (2007). Nitric oxide reductase (*norB*) gene sequence analysis reveals discrepancies with nitrite reductase (*nir*) gene phylogeny in cultivated denitrifiers. Environmental Microbiology, 9(4): 1072–1077

Higgins S A, Welsh A, Orellana L H, Konstantinidis K T, Chee-Sanford J C, Sanford R A, Schadt C W, Löffler F E (2016). Detection and diversity of fungal nitric oxide reductase genes (*p450nor*) in agricultural soils. Applied and Environmental Microbiology, 82(10): 2919–2928

Hu H W, Chen D, He J Z (2015). Microbial regulation of terrestrial nitrous oxide formation: understanding the biological pathways for prediction of emission rates. FEMS Microbiology Reviews, 39(5): 729–749

Hu Z, Wessels H J C T, van Alen T, Jetten M S M, Kartal B (2019). Nitric oxide-dependent anaerobic ammonium oxidation. Nature Communications, 10(1): 1244

Ishii S, Song Y, Rathnayake L, Tumendelger A, Satoh H, Toyoda S, Yoshida N, Okabe S (2014). Identification of key nitrous oxide production pathways in aerobic partial nitrifying granules. Environmental Microbiology, 16(10): 3168–3180

Jamali M A M, Gopalasingam C C, Johnson R M, Tosha T, Muramoto K, Muench S P, Antonyuk S V, Shiro Y, Hasnain S S (2020). The active form of quinol-dependent nitric oxide reductase from *Neisseria meningitidis* is a dimer. IUCrJ, 7(3): 404–415

Kahle M, ter Beek J, Hosler J P, Ädelroth P (2018). The insertion of the non-heme FeB cofactor into nitric oxide reductase from P. denitrificans depends on *norq* and *nord* accessory proteins. Biochimica et Biophysica Acta (BBA). Bioenergetics, 1859(10): 1051–1058

Kearse M, Moir R, Wilson A, Stones-Havas S, Cheung M, Sturrock S, Buxton S, Cooper A, Markowitz S, Duran C, Thierer T, Ashton B, Meintjes P, Drummond A (2012). Geneious Basic: An integrated and extendable desktop software platform for the organization and analysis of sequence data. Bioinformatics (Oxford, England), 28(12): 1647–1649

Kumar S, Stecher G, Tamura K (2016). MEGA7: Molecular Evolutionary Genetics Analysis version 7.0 for bigger datasets. Molecular Biology and Evolution, 33(7): 1870–1874

Kuypers M M M, Marchant H K, Kartal B (2018). The microbial nitrogen-cycling network. Nature Reviews. Microbiology, 16(5): 263–276

Lewis A M, Matzdorf S S, Endres J L, Windham I H, Bayles K W, Rice K C (2015). Examination of the *Staphylococcus aureus* nitric oxide reductase (*saNOR*) reveals its contribution to modulating intracellular NO levels and cellular respiration. Molecular Microbiology, 96(3): 651–669

Li W, Li H, Liu Y, Zheng P, Shapleigh J P (2018). Salinity-aided selection of progressive onset denitrifiers as a means of providing nitrite for anammox. Environmental Science & Technology, 52(18): 10665–10672

Liu Y, Peng L, Ngo H H, Guo W, Wang D, Pan Y, Sun J, Ni B J (2016). Evaluation of nitrous oxide emission from sulfide- and sulfur-based autotrophic denitrification processes. Environmental Science & Technology, 50(17): 9407–9415

Ma Y, Zilles J L, Kent A D (2019). An evaluation of primers for detecting denitrifiers via their functional genes. Environmental Microbiology, 21(4): 1196–1210

Matsumoto Y, Tosha T, Pisliakov A V, Hino T, Sugimoto H, Nagano S, Sugita Y, Shiro Y (2012). Crystal structure of quinol-dependent nitric oxide reductase from *Geobacillus stearothermophilus*. Nature Structural & Molecular Biology, 19(2): 238–245

Meyer R L, Zeng R J, Giugliano V, Blackall L L (2005). Challenges for simultaneous nitrification, denitrification, and phosphorus removal in microbial aggregates: Mass transfer limitation and nitrous oxide production. FEMS Microbiology Ecology, 52(3): 329–338

Moroz L L, Kohn A B (2011). Parallel evolution of nitric oxide signaling: Diversity of synthesis & memory pathways. Frontiers in Bioscience, 16(1): 2008–2051

Myung J, Wang Z, Yuan T, Zhang P, Van Nostrand J D, Zhou J, Criddle C S (2015). Production of nitrous oxide from nitrite in stable Type II methanotrophic enrichments. Environmental Science & Technology, 49(18): 10969–10975

National Academy of Engineering (2016). Grand Challenges for Engineering: Imperatives, Prospects, and Priorities: Summary of a Forum. Washington, DC: The National Academies Press

Navarro-González R, Molina M J, Molina L T (1998). Nitrogen fixation by volcanic lightning in the early Earth. Geophysical Research Letters, 25(16): 3123–3126

Onley J R, Ahsan S, Sanford R A, Löffler F E (2018). Denitrification by *Anaeromyxobacter dehalogenans*, a common soil bacterium lacking the nitrite reductase genes *nirS* and *nirK*. Applied and Environmental Microbiology, 84(4): e01985–17

Overbeek R, Olson R, Pusch G D, Olsen G J, Davis J J, Disz T, Edwards R A, Gerdes S, Parrello B, Shukla M, Vonstein V, Wattam A R, Xia F, Stevens R (2014). The SEED and the Rapid Annotation of microbial genomes using Subsystems Technology (RAST). Nucleic Acids Research, 42(D1): D206–D214

Parks D H, Imelfort M, Skennerton C T, Hugenholtz P, Tyson G W (2015). CheckM: Assessing the quality of microbial genomes recovered from isolates, single cells, and metagenomes. Genome Research, 25(7): 1043–1055

Philippot L (2002). Denitrifying genes in bacterial and Archaeal genomes. Biochimica et Biophysica Acta (BBA), 1577(3): 355–376

Santana M M, Gonzalez J M, Cruz C (2017). Nitric oxide accumulation: The evolutionary trigger for phytopathogenesis. Frontiers in Microbiology, 8: 1947

Schalk-Otte S (2000). Nitrous oxide (N_2O) production by *Alcaligenes faecalis* during feast and famine regimes. Water Research, 34(7): 2080–2088

Scherson Y D, Criddle C S (2014). Recovery of freshwater from wastewater: Upgrading process configurations to maximize energy recovery and minimize residuals. Environmental Science & Technology, 48(15): 8420–8432

Scherson Y D, Wells G F, Woo S G, Lee J, Park J, Cantwell B J, Criddle C S (2013). Nitrogen removal with energy recovery through N_2O decomposition. Energy & Environmental Science, 6(1): 241–248

Scherson Y D, Woo S G, Criddle C S (2014). Production of nitrous oxide from anaerobic digester centrate and its use as a co-oxidant of biogas to enhance energy recovery. Environmental Science & Technology, 48(10): 5612–5619

Schreiber F, Wunderlin P, Udert K M, Wells G F (2012). Nitric oxide and nitrous oxide turnover in natural and engineered microbial communities: Biological pathways, chemical reactions, and novel technologies. Frontiers in Microbiology, 3: 372

Seemann T (2014). Prokka: Rapid prokaryotic genome annotation. Bioinformatics (Oxford, England), 30(14): 2068–2069

Shan J, Sanford R A, Chee-Sanford J, Ooi S K, Löffler F E, Konstantinidis K T, Yang W H (2021). Beyond denitrification: The role of microbial diversity in controlling nitrous oxide reduction and soil nitrous oxide emissions. Global Change Biology, 27(12): 2669–2683

Stanton C L, Reinhard C T, Kasting J F, Ostrom N E, Haslun J A, Lyons T W, Glass J B (2018). Nitrous oxide from chemodenitrification: A possible missing link in the *Proterozoic* greenhouse and the evolution of aerobic respiration. Geobiology, 16(6): 597–609

Stein L Y, Campbell M A, Klotz M G (2013). Energy-mediated vs. ammonium-regulated gene expression in the obligate ammonia-oxidizing bacterium, Nitrosococcus oceani. Frontiers in Microbiology, 4: 277

Terasaka E, Yamada K, Wang P H, Hosokawa K, Yamagiwa R, Matsumoto K, Ishii S, Mori T, Yagi K, Sawai H, Arai H, Sugimoto H, Sugita Y, Shiro Y, Tosha T (2017). Dynamics of nitric oxide controlled by protein complex in bacterial system. Proceedings of the National Academy of Sciences of the United States of America, 114(37): 9888–9893

Thompson J D, Gibson T J, Plewniak F, Jeanmougin F, Higgins D G (1997). The CLUSTAL_X windows interface: Flexible strategies for multiple sequence alignment aided by quality analysis tools. Nucleic Acids Research, 25(24): 4876–4882

Tian H, Xu R, Canadell J G, Thompson R L, Winiwarter W, Suntharalingam P, Davidson E A, Ciais P, Jackson R B, Janssens-Maenhout G, Prather M J, Regnier P, Pan N, Pan S, Peters G P, Shi H, Tubiello F N, Zaehle S, Zhou F, Arneth A, Battaglia G, Berthet S, Bopp L, Bouwman A F, Buitenhuis E T, Chang J, Chipperfield M P, Dangal S R S, Dlugokencky E, Elkins J W, Eyre B D, Fu B, Hall B, Ito A, Joos F, Krummel P B, Landolfi A, Laruelle G G, Lauerwald R, Li W, Lienert S, Maavara T, MacLeod M, Millet D B, Olin S, Patra P K, Prinn R G, Raymond P A, Ruiz D J, van der Werf G R, Vuichard N, Wang J, Weiss R F, Wells K C, Wilson C, Yang J, Yao Y (2020). A comprehensive quantification of global nitrous oxide sources and sinks. Nature, 586(7828): 248–256

Verbaendert I, Hoefman S, Boeckx P, Boon N, De Vos P (2014). Primers for overlooked *nirK, qnorB*, and *nosZ* genes of thermophilic Gram-positive denitrifiers. FEMS Microbiology Ecology, 89(1): 162–180

Wang Z, Woo S G, Yao Y, Cheng H H, Wu Y J, Criddle C S (2020). Nitrogen removal as nitrous oxide for energy recovery: Increased process stability and high nitrous yields at short hydraulic residence times. Water Research, 173: 115575

Weißbach M, Thiel P, Drewes J E, Koch K (2018). Nitrogen removal and intentional nitrous oxide production from reject water in a coupled nitritation/nitrous denitritation system under real feed-stream conditions. Bioresource Technology, 255: 58–66

Woehle C, Roy A S, Glock N, Wein T, Weissenbach J, Rosenstiel P, Hiebenthal C, Michels J, Schönfeld J, Dagan T (2018). A novel eukaryotic denitrification pathway in foraminifera. Current Biology, 28(16): 2536–2543.e5

Zhu B, Bradford L, Huang S, Szalay A, Leix C, Weissbach M, Táncsics A, Drewes J E, Lueders T (2017). Unexpected diversity and high abundance of putative nitric oxide dismutase (*Nod*) genes

in contaminated aquifers and wastewater treatment systems. Applied and Environmental Microbiology, 83(4): e02750–e16

Zhu B, Wang J, Bradford L M, Ettwig K, Hu B, Lueders T (2019). Nitric oxide dismutase (*nod*) genes as a functional marker for the diversity and phylogeny of methane-driven oxygenic denitrifiers. Frontiers in Microbiology, 10: 1577

Zhuge Y, Shen X, Liu Y, Shapleigh J, Li W (2020). Application of acidic conditions and inert-gas sparging to achieve high-efficiency nitrous oxide recovery during nitrite denitrification. Water Research, 182: 116001

Zumft W (2005). Nitric oxide reductases of prokaryotes with emphasis on the respiratory, heme-copper oxidase type. Journal of Inorganic Biochemistry, 99(1): 194–215